15 January 1999

ELSEVIER

Optics Communications 159 (1999) 221–224

OPTICS COMMUNICATIONS

# De-excitation mechanisms of $BaLiF_3:Co^{2+}$ crystals

Marcos Duarte [1], Evely Martins [2], Sônia L. Baldochi, Nilson D. Vieira Jr., Martha M.F. Vieira *

*Instituto de Pesquisas Energéticas e Nucleares, P.O. Box 11049, 05422-970 São Paulo, SP, Brazil*

Received 20 October 1998; accepted 10 November 1998

**Abstract**

The de-excitation mechanisms from the $^4T_2(^4F)$ level for a promising new vibronic laser material, $BaLiF_3:Co^{2+}$ (emission centered at 1588 nm, FWHM = 426 nm), are reported. At low temperatures, the decay time is on average equal to 580 μs, decreasing very rapidly above 80 K ($\tau_{RT} = 1$ μs). This decrease is due to multiphonon processes from the excited vibronic level $^4T_2(^4F)$ to the highly excited vibronic fundamental level $^4T_1(^4F)$ promoted by the vibrational modes $E_g$ and $T_{2g}$ of the $BaLiF_3$ crystal. The decay time dependence on the temperature was fitted according to the Mott–Seitz model, presenting a good agreement. The following parameters were determined: radiative lifetime, $\tau_R = 580$ μs, nonradiative lifetime, $\tau_{NR} = 0.17$ μs and activation energy, $\Delta E = 587$ cm$^{-1}$. 

*PACS:* 78.50.W
*Keywords:* Optical materials; Luminescence; Optical properties

## 1. Introduction

There has been considerable interest in developing laser active media with broadband emission for applications such as ultrashort pulse generation and tunability, particularly in the 1500-nm spectral region that coincides with the third-telecommunication window.

The absorption spectroscopic properties of the transition metal ions $Ni^{2+}$ [1,2] and $Co^{2+}$ [2,3] and the de-excitation mechanisms of $Ni^{2+}$ [4] in the new matrix $BaLiF_3$ have been reported recently. These ions, due to their vibronic characteristic of emission, are potentially tunable laser active media over a range of hundreds of nanometers in the 1500-nm spectral region. Although laser operation for $Co^{2+}$ and $Ni^{2+}$ ions in many crystal hosts has been reported [5–9], as far as we are concerned laser action has not yet been observed for a transition metal ion in the $BaLiF_3$ matrix.

In $BaLiF_3:Co^{2+}$ crystals, the $BaLiF_3$ matrix presents an 'inverse' perovskite structure where the $Co^{2+}$ ions are located in octahedral sites [2]. This system presents two intense absorption bands, one peaking at 20 000 cm$^{-1}$ (500 nm), corresponding to $^4T_1(^4F) \rightarrow {}^4T_1(^4P)$ transition and the other peaking at 8264 cm$^{-1}$ (1210 nm), corresponding to $^4T_1(^4F) \rightarrow {}^4T_2(^4F)$ transition, with bandwidths around 20%. A weaker band was also observed at 16 667 cm$^{-1}$ (600 nm), corresponding to the $^4T_1(^4F) \rightarrow {}^4A_2(^4F)$ transition. $BaLiF_3:Co^{2+}$ shows a single emission band, centered at 6297 cm$^{-1}$ (1588 nm), corresponding to the transition $^4T_2(^4F) \rightarrow {}^4T_1(^4F)$, with a meaningful 426 nm full width at half maximum (FWHM), at room temperature [3].

The investigation of the de-excitation mechanisms is crucial to understand and establish the spectroscopic condi-

* E-mail: mmviera@net.ipen.br
[1] Present address: Escola de Educação Física, Universidade de São Paulo, São Paulo, SP, Brazil. E-mail: mduarte@usp.br
[2] Present address: Instituto Tecnológico de Aeronáutica, ITA, Sao José dos Campos, SP, Brazil. E-mail: evely@ele.ita.cta.br

0030-4018/99/$ - see front matter 
PII: S0030-4018(98)00616-6

tions for laser operation of a candidate to laser active medium. In this work, we report the decay time and the luminescent emission intensity dependences on temperature for $Co^{2+}$ ions in the $BaLiF_3$ host.

## 2. Experimental

The studied $BaLiF_3$:$Co^{2+}$ crystals were grown at our laboratories by the Czochralski technique [2]. Two crystals with different cobalt concentrations, determined by neutron activation analysis [2] were used in our measurements: 0.05 and 0.44 mol% in the boule. For the decay time and luminescence intensity measurements, a conventional set up with a perpendicular geometry and AC lock-in technique was used to maximize the signal-to-noise ratio. The samples were placed in a commercial closed cycle helium cryostat (Displex Cs-200, Air Products), that allows operation from 10 to 300 K.

The $^4T_1(^4F) \rightarrow {}^4T_1(^4P)$ transition (peaking at 500 nm) was excited by an argon ion laser (488 nm and 514.5 nm, 3 W – Spectra Physics 171) or by a pulsed dye laser operating at 10 Hz, with a beam rise time of 500 ns and pulse rate of 100 μs (471–577 nm, Coumarin C-503, Laser Photonics). The $^4T_1(^4F) \rightarrow {}^4T_2(^4F)$ transition (peaking at 1210 nm) was excited by a Nd:YAG laser (1064 nm, 0.5 W – Quantronix).

In order to produce a narrow pulsed beam, the continuous beam of the argon ion or the ND:YAG laser was focused into a designed chopper blade. The variation of the chopper frequency allowed pulses with the desired characteristics for excitation to be obtained. At the maximum chopper frequency, the rise time of the obtained beam was shorter than 3.2 μs and with a pulse period of 1 ms. Even using this apparatus, the measurement of the decay time was possible only up to 200 K. For the $^4T_1(^4F) \rightarrow {}^4T_1(^4P)$ transition (peaking at 500 nm) we used the pulsed dye laser for excitation above 200 K.

The integrated emission was collected by an InSb diode detector, cooled at 77 K (Judson Infrared) with response time less than 1 μs, and the signal was processed by a Boxcar integrator (PAR 4402).

## 3. Results and discussion

The dependence on the temperature of luminescent decay time, $\tau(T)$, for an ion in a crystal, using the Mott–Seitz model [10], is given by:

$$\frac{1}{\tau(t)} = \frac{1}{\tau_R(T)} + \frac{1}{\tau_{NR}^0 \exp(\Delta E/KT)}, \quad (1)$$

where $\tau_R(T)$ is the radiative decay time of the luminescent ion, $K$ is the Boltzmann constant and $\Delta E$ is the activation energy that will be defined afterwards. The second term on the right side is the nonradiative decay time of the luminescent ion, $\tau_{NR}(T)$, following the Mott–Seitz model [10], where the temperature dependence of $\tau_{NR}(T)$, can be described by a single Arrhenius factor related to the occupation probability of the electrons in the vibrational excited state. For the transition metal ion $Co^{2+}$, the nonradiative processes result from multiphonon emission from the excited vibronic level $^4T_2(^4F)$ to the highly excited vibronic fundamental level $^4T_1(^4F)$. The activation energy, $\Delta E$, is the energy difference between the ground state of the $^4T_1$ level and the crossover of the potential energy surfaces of the $^4T_1$ and $^4T_2$ levels. Therefore, if the decay is a single exponential and the optical absorption intensity is independent of the crystal temperature (pumping at 500 nm and at 1064 nm, with a temperature range from 10 K to RT, the decrease in the optical absorption is less than 5%), the integrated luminescent intensity $I(T)$ is given by [11]:

$$I(T) = I_0 \frac{\tau(T)}{\tau_R(T)}. \quad (2)$$

Thus, the ratio $R(T)$ of the normalized decay time, for a normalized intensity, is given by:

$$R(T) = \frac{\tau(T)/\tau(0)}{I(T)/I(0)} = \frac{\tau_R(T)}{\tau_R(0)}. \quad (3)$$

The ratio $R(T)$ allows one to determine the influence of temperature on the radiative decay time. Experimentally, if the ratio $R(T)$ is temperature independent, and thus $\tau_R(T)$ is independent as well, then the decrease of decay time with the temperature can be completely attributed to nonradiative processes. Experimentally, the ratio $R(T)$ can be determined and the temperature dependence of the decay time curves can be fitted by a convenient function. For $BaLiF_3$:$Co^{2+}$ the ratio $R(T)$ obtained is temperature independent, within a range of 20% of variation that can be explained as an experimental error. Thus, the decay time can be given by Eq. (1), and the only temperature dependent term is the nonradiative decay:

$$\tau(T) = \frac{\tau_R}{1 + (\tau_R/\tau_{NR}^0)\exp(-\Delta E/KT)}. \quad (4)$$

Fig. 1 shows the luminescent decay time dependence on the temperature for $Co^{2+}$ ions in $BaLiF_3$ pumping at the two main absorption bands. The same behaviour with temperature is observed by pumping with the 1064 nm Nd:YAG laser line that overlaps the 1210 nm band ($^4T_1(^4F) \rightarrow {}^4T_2(^4F)$ transition), and with the 500 nm dye laser line that overlaps the 500 nm band ($^4T_1(^4F) \rightarrow {}^4T_1(^4P)$ transition). The temporal behaviors of the luminescent decay time for excitation in both bands present single exponential decays for all studied temperatures. From the above statements, it is evident that the transitions have the same single channel of de-excitation. A single emission band in the infrared region is characteristic of $Co^{2+}$ ions

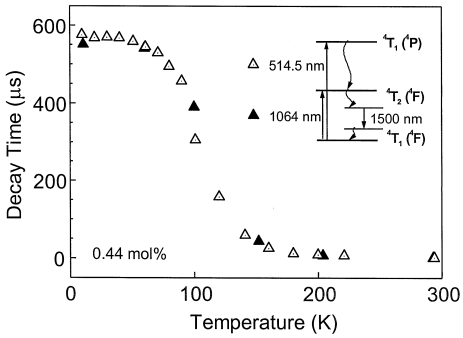


Fig. 1. Luminescent decay time pumping at the two main absorption bands ($BaLiF_3:Co^{2+}$, 0.44 mol%) and energy level diagram in the studied region.

in octahedral symmetry [12]. The corresponding energy levels diagram for the studied optical transitions can be observed in Fig. 1.

Figs. 2 and 3 present the decay times, their fits by Eq. (4), the luminescence intensity curves, and the ratio $R(T)$ (Eq. (3)), for the sample with 0.05 mol% and 0.44 mol% $Co^{2+}$ concentration in $BaLiF_3$, respectively. The results in Figs. 2 and 3 are shown for the 500-nm excitation (dye laser). The parameters obtained by the theoretical fit (Mott–Seitz model) for the two $Co^{2+}$ concentrations in the $BaLiF_3$ crystal are listed in Table 1.

As one can observe in Figs. 2 and 3, the decay time and the luminescent intensity behaviour for both samples are similar and decrease at the same temperature, around 80 K. This demonstrates that the nonradiative de-excitation mechanism involved in the decrease of the decay time has an activation temperature independent of $Co^{2+}$ concentration, which is confirmed by the $\Delta E$ values shown in Table 1. The $Co^{2+}$ ion can be considered isolated in the matrix (the studied samples have a very low $Co^{2+}$ concentration).

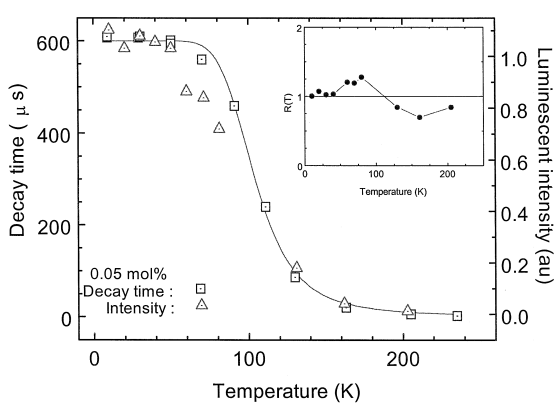


Fig. 2. Luminescent decay time and intensity and $R(T)$ (inset), ratio of the relative luminescent decay time and relative total luminescent intensity (Eq. (3)) (see text) ($BaLiF_3:Co^{2+}$, 0.44 mol%). Line: fitted by Eq. (4) (see text).

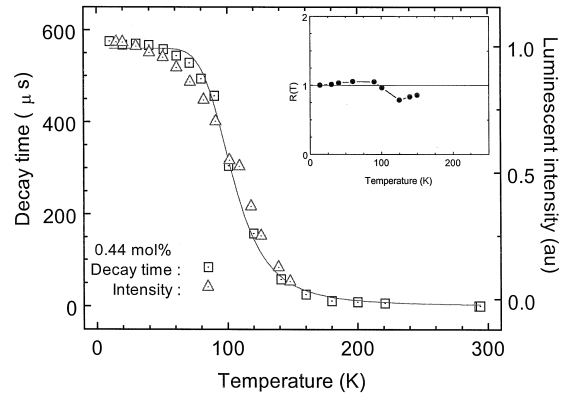


Fig. 3. Luminescent decay time and intensity and $R(T)$ (inset), ratio of the relative luminescent decay time and relative total luminescent intensity (Eq. (3)) (see text) ($BaLiF_3:Co^{2+}$, 0.05 mol%). Line: fitted by Eq. (4) (see text).

This result was expected once this process is simply a probability factor of occupation of the electron in the excited state.

The strong dependence of the luminescent decay time on temperature can be explained, since $\Delta E$ (the potential barrier energy for one electron to change from the excited level $^4T_2(^4F)$ to the highly excited vibronic fundamental level $^4T_1(^4F)$) is on average 587 $cm^{-1}$ and the phonon density of state energy peaks at 509 $cm^{-1}$ [13]. Consequently, roughly only one phonon mode is necessary to overcome the potential barrier and allow for nonradiative decay. Because the excitation of the vibronic level is highly dependent on temperature, a fast onset of the nonradiative decay with temperature increase was expected.

The long radiative lifetime measured for $BaLiF_3:Co^{2+}$ was predictable, since the octahedral symmetry induces smaller oscillator strength among $3d^n$ states [14]. This can happen because the ion sites show inversion symmetry. Tetrahedrical sites, on the other hand, do not have inversion symmetry, conducing to a bigger opposite parity electronic configuration mix and consequently produce a bigger oscillator strength [15]. Higher oscillator strength conduces to shorter lifetimes. The radiative lifetimes usually found in octahedral symmetry are in the range of milliseconds. Although, when $BaLiF_3:Co^{2+}$ is compared to other $Co^{2+}$ doped hosts, as shown in Table 2, the shortening of lifetime observed indicates a perturbation in the octahedral site, as reported in a previous study [3]. This

Table 1
Parameters giving the temperature dependence of the fluorescence lifetime ($BaLiF_3:Co^{2+}$, 0.05 and 0.44 mol%)

| $c$ (mol%) | $\tau_R$ (μs) | $\tau_{NR}^{o}$ (μs) | $\Delta E$ ($cm^{-1}$) | $\tau_{RT}$ (μs) |
|---|---|---|---|---|
| 0.05 | 600(5) | 0.15(8) | 599(38) | – |
| 0.44 | 560(5) | 0.20(8) | 575(28) | 1.0(5) |

Table 2
Decay time for $Co^{2+}$ doped fluoperovskites and for $BaLiF_3:Ni^{2+}$ (infrared transition)

| | $BaLiF_3:Co^{2+}$ | $KMgF_3:Co^{2+}$ [12] | $KZnF_3:Co^{2+}$ [18] | $BaLiF_3:Ni^{2+}$ [4] |
|---|---|---|---|---|
| $\tau_R$(10 K) | 600 μs | 2.5 ms | 800 μs | 5 ms |
| $\tau$(300 K) | 1 μs | 200 μs | 25 μs | 2 ms |

perturbation might be due to charge compensation mechanisms, but the exact cause of this perturbation remains unknown.

The decay time dependence on temperature for the infrared transition in $BaLiF_3:Ni^{2+}$, is not as strong as for $BaLiF_3:Co^{2+}$, as shown in Table 2. The decay time shortening as the temperature rises is a consequence of the increase of the nonradiative components in the de-excitation process, which is a consequence of multiphononic processes for both ions. The lattice phonons present the symmetry of the crystal vibrational modes. For cubic symmetry the even symmetry modes $A_{1g}$, $E_g$, and $T_{2g}$ and the odd symmetry modes $T_{1u}$, $T_{1u}$, and $T_{2u}$ are possible [16]. As the nonradiative transition connects even symmetric states for $Co^{2+}$ ($^4T_{2g} \rightarrow {}^4T_{1g}$) and $Ni^{2+}$ ($^3T_{2g} \rightarrow {}^3A_{2g}$), the odd vibrational modes are discarded immediately. The product of the excited state representations of both ions by the vibrational mode representations provides the vibrational modes responsible for the promotion of the transition. Because of this product for $BaLiF_3:Ni^{2+}$ there is no vibrational mode connecting the states $^3T_{2g}$ and $^3A_{2g}$ and a long decay time is observed at all temperatures [4]. On the other hand, for $BaLiF_3:Co^{2+}$, the vibrational modes $E_g$ and $T_{2g}$ act as promoting modes of the nonradiative transition between the states $^4T_{2g}$ and $^4T_{1g}$. Consequently, the multiphononic emission rate to the $Co^{2+}$ ion is much bigger than for the $Ni^{2+}$ ion in this system. Similar observation was reported by Robbins and Thompson [17] for $Co^{2+}$ and $Ni^{2+}$ ions in other hosts.

## 4. Conclusion

The decay time at low temperatures of $BaLiF_3:Co^{2+}$ is on average 580 μs, and at room temperature is 1.0 μs. The high dependence of the decay time on the temperature is explained, using the Mott–Seitz model, due in part to the small potential barrier energy, $\Delta E$. With temperature increase, multiphonon processes from the excited vibronic level $^4T_2(^4F)$ to the highly excited vibronic fundamental level $^4T_1(^4F)$ were promoted by the vibrational modes $E_g$ and $T_{2g}$ of the $BaLiF_3$ crystal, diminishing the luminescent decay time. The decay time behaviour observed was independent of $Co^{2+}$ concentration in the samples, thus pair effects are not considered.

Considering the de-excitation mechanisms and the optical spectroscopic parameters for $BaLiF_3:Co^{2+}$, the first calculations for laser tests indicate that laser operation will be possible only at low temperature (up to 80 K).

## Acknowledgements

We acknowledge CNPQ/RHAE and FAPESP for scholarships for M. Duarte and E. Martins, respectively. This work was partially supported by FAPESP.

## References

[1] E. Martins, N.D. Vieira Jr., S.L. Baldochi, S.P. Morato, J.Y. Gesland, J. Lumin. 62 (1994) 281.
[2] S.L. Baldochi, A.M.E. Santo, E. Martins, M. Duarte, M.M.F. Vieira, N.D. Vieira Jr., S.P. Morato, J. Cryst. Growth 166 (1996) 375.
[3] M. Duarte, E. Martins, S.L. Baldochi, S.P. Morato, N.D. Vieira Jr., M.M.F. Vieira, Optics Commun. 151 (1998) 366.
[4] Martins, M. Duarte, S.L. Baldochi, S.P. Morato, M.M.F. Vieira, N.D. Vieira Jr., J. Phys. Chem. Solids 58 (1997) 655.
[5] M.V. Iverson, W.A. Sibley, J. Lumin. 20 (1979) 311.
[6] L.F. Mollenauer, J.C. White, in: Tunable Lasers Topics in Applied Physics, Vol. 59, Springer Series, New York, 1987.
[7] Penzkoffer, in: Solid State Lasers, Prog. Quant. Elect., Vol. 12, Pergamon, UK, 1988.
[8] P.F. Moulton, IEEE J. Quantum. Electron. QE-18 (1982) 1185.
[9] Villacampa, R. Cases, V.M. Orera, R. Alcalá, J. Phys. Chem. Solids 55 (1994) 263.
[10] B. Canny, D. Curie, in: B. Di Bartolo (Ed.), Advances in Nonradiative Processes in Solids, Series B: Physics, Vol. 249, Plenum, New York, 1989.
[11] M. Stalder, M. Bass, B.H.T. Chai, J. Opt. Soc. Am. B 9 (1992) 2271.
[12] D. Sturge, Phys. Rev. B 8 (1973) 6.
[13] A. Boumriche, P. Simon, M. Rousseau, J.Y. Gesland, F. Gervais, J. Phys.: Condens. Matter 1 (1989) 5613.
[14] J. Fergusson, D.L. Wood, K. Knox, J. Chem. Phys. 39 (1963) 881.
[15] J.R. Caird, Tunable Solid-State Lasers, in: A.B. Budgor, L. Esterowitz, L.G. DeShazer (Eds.), Springer Verlag, New York, 1986, p. 20.
[16] Di Bartolo, Optical Interactions in Solids, Wiley, New York, 1968.
[17] J. Robbins, A.J. Thompson, Mol. Phys. 25 (1973) 1103.
[18] N.L. Rowell, D.J. Lockwood, J. Electrochem. Soc. 136 (1989) 3536.